TI Designs
Variable Threshold Hall Proximity Sensor with PNP or NPN

TI Designs

TI Designs provide the foundation that you need including methodology, testing and design files to quickly evaluate and customize the system. TI Designs help *you* accelerate your time to market.

Design Resources

TIDA-00286	Tool Folder Containing Design Files
DRV5053	Product Folder
MSP430FR5738	Product Folder
SN65HVD101	Product Folder

TI E2E™ Community

ASK Our E2E Experts
WEBENCH® Calculator Tools

Design Features

- Magnetic Field Proximity Sensor
- Switched Output (PNP or NPN)
- Configurable Threshold (Through Onboard Button)

Featured Applications

- Factory Automation and Process Control
- Building Automation
- Sensors and Field Transmitters
- Portable Instrumentation

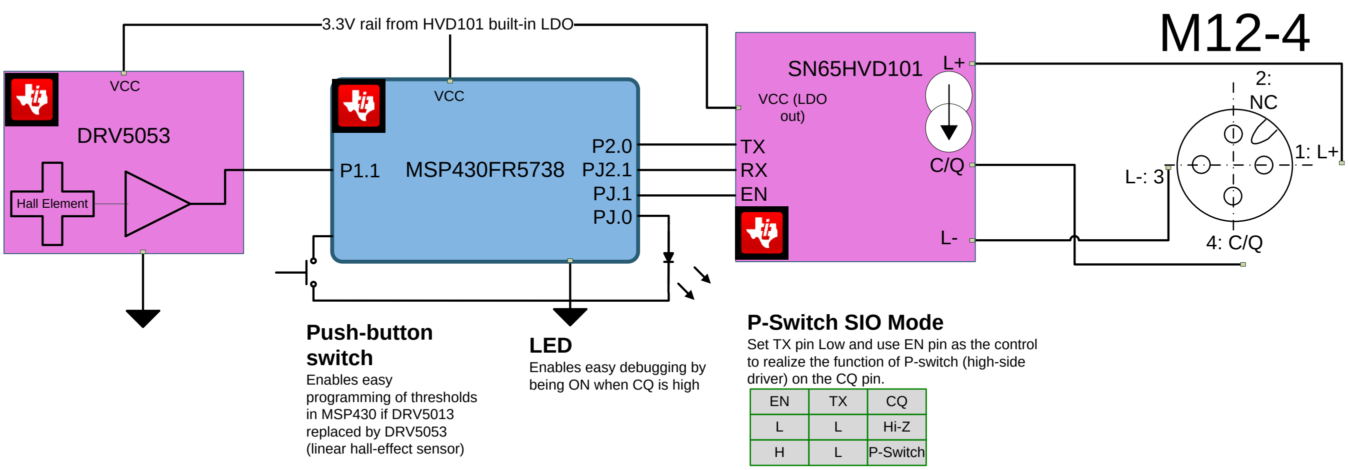

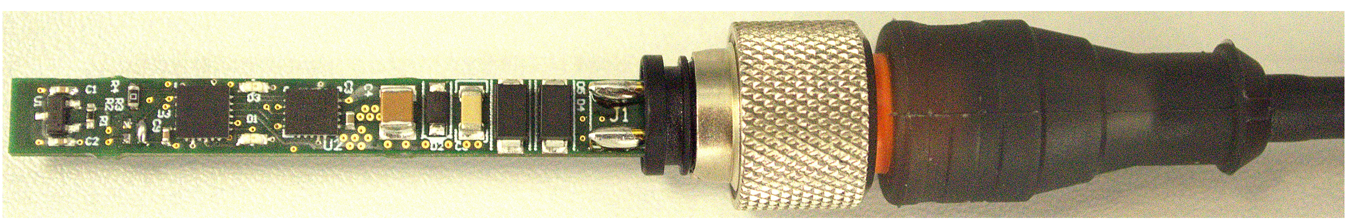

An IMPORTANT NOTICE at the end of this TI reference design addresses authorized use, intellectual property matters and other important disclaimers and information.

1 Key System Specifications

Table 1. Key System Specifications

PARAMETER	SPECIFICATION	VALUE	DETAILS
VCC	Nominal operating voltage	24.0 V	Section 3.3
Iq	Nominal operating current	5 mA (LED OFF) 7.5 mA (LED ON)	Section 7.3
Iout	Output current	250 mA	Section 3.3
Vdrop	Voltage drop	<2.5 V	Section 3.3
PNP_NPN	Switching output	PNP (NPN settings possible)	Section 5.1
NO_NC	Switching function	NO (NC settings also possible)	Section 5.1
Ta	Temperature range	–40°C to 85°C	Section 3.4
	Form factor	M12	Section 8.2
	Connections	M12	Section 8.2
	Switching frequency	<20 kHz	Section 3.2
	Number of resolved positions	50	Section 4.3
	Reverse protection	Yes	Section 3.3

2 System Design Theory

2.1 Physics Refresher for Hall Effect

The Hall effect is based on the influence of a magnetic field on moving charge carriers. The principle was discovered by Edwin Hall in 1879 and is now widely used in all kinds of applications. See Reference 8 for an explanation on the working principle of a Hall sensor.

A potential difference between the two opposite ends of the long side of the conductor builds up an electric field

$$\vec{F}_{el} = q\vec{E} \tag{1}$$

Therefore, *q* is the elementary charge that can either be of positive or negative sign. The electric field *E* is connected to the velocity *v* of the charge carriers and to the current density *J* through Equation 2 and Equation 3. The charge carriers are characterized by the electron charge *q*, the charge carrier mobility *μ*, and the charge carrier density *N* inside the conducting material.

$$\vec{v} = \mu\vec{E} \tag{2}$$

$$\vec{J} = q\mu N\vec{E} \tag{3}$$

If a magnetic field is present the magnetic force F_{mag} acts on the charge carriers, too. Only negative charge carriers contribute to the current. The influence of the magnetic force depends on the magnetic flux density *B* and the velocity *v* of the charge carriers. The force acts perpendicular to *v* and distracts the charge carriers from their straight moving direction from one electrode to the other in a specific angle and is defined by Equation 4

$$\vec{F}_{mag} = q\left(\vec{v} \times \vec{B}\right) \tag{4}$$

As a consequence to the influence of the magnetic force, a counterbalancing Hall electric field *E_H* builds up. Using Equation 1 to Equation 3 in Equation 4 *E_H* can be rewritten as Equation 5

$$\vec{E}_H = -\left(\vec{v} \times \vec{B}\right) = -\mu\left(\vec{E} \times \vec{B}\right) = -\frac{1}{qN}\left(\vec{J} \times \vec{B}\right) \tag{5}$$

The distraction angle *Theta_H* from the moving direction can then be described as Equation 6

$$\theta_H = \arctan\left(\frac{\left|\vec{E}_H\right|}{E_x}\right) \tag{6}$$

The potential difference due to the magnetic force can be measured at the ends of the conductor perpendicular to the applied voltage. Using Equation 7:

$$\vec{J} = \frac{\vec{I}}{wt} \quad \text{and} \quad \vec{E} = \frac{\vec{V}}{w} \tag{7}$$

Equation 5 can be rearranged to the common expression for the Hall voltage Equation 8

$$V_H = \frac{1}{qN}\frac{I_x}{t}B_z = R_H\frac{I_x}{t}B_z \tag{8}$$

R_H is defined as the Hall resistance of the conductor (see Reference 6). Although this cannot be seen directly from Equation 7, it is important to note that the factor defining the Hall voltage sensitivity is the charge carrier mobility μ. Therefore, the equation is rewritten in dependence of the applied voltage V_x (see Reference 8) as Equation 9:

$$V_H = \frac{1}{qN}\frac{I_x}{t}B_z = \frac{1}{qNt}\frac{V_x}{R}B_z = \frac{1}{qNt}\frac{tw}{pl}V_xB_z = \frac{1}{qN}\frac{wqN\mu}{l}V_xB_z = \frac{w}{l}\mu V_xB_z \tag{9}$$

In this equation, *R* refers to the resistance of the conducting material and must not be mistaken for the Hall resistance *R_H* in Equation 8.

2.2 Specifics for Disc Magnets

The static magnetic field of a disc magnet is dependent on its magnetic remanence B_r, height h, and radius r. The magnetic flux density at a certain distance z from the surface of the magnet is calculated to

$$B(z)=\frac{B_r}{2}\left[\frac{h+z}{\sqrt{r^2+(h+z)^2}}-\frac{z}{\sqrt{r^2+z^2}}\right]$$

where

- B_r is the magnetic remanence
- h is the height
- r the radius of the disc magnet (10)

The magnetic field strength is equal for both distances in either direction of the disc magnet. Only the magnetic field lines are orientated oppositely. Depending on the orientation of the magnet, compared to the electric field inside the conductor, the measured Hall voltage \index{Hall voltage} is either of positive or negative sign.

2.3 Simulating Magnetic Field for System Design

Though many tools can be used to simulate magnetic field, this section details using the tool called femm 4.2 [7]. This tool uses the finite element method to calculate magnetic fields. The finite element method is a numerical method to calculate solutions for partial differential equations. In principle, the area in which the magnetic field is propagating is divided into several small elements with finite size. For every element a basic function is defined. Together with boundary and transition conditions, these basic functions are inserted into the general partial differential equation. Then, the resulting system of equations is solved numerically. A detailed equation about the dinfite element method can be found in *The Finite Element Method* [9]. To explain the handling of the tool, consider Figure 1. Femm 4.2 calculates the magnetic field for axis symmetric objects the y axis serves as rotation axis. A complete documentation of the toll can be found online at www.femm.info.

First, the user has to define the dimensions of the magnet and its surrounding area. The box on the left side in Figure 1 is the magnet, the outer area is air. Second, the properties of the defined areas must be set. In this case, the orientation of the magnetization direction is set to 90° and the coercive field strength Hc is set to 925 kA/m. For the surrounding area, no specific parameters are set. Now, the magnetic field can be simulated. The result is shown Figure 1. The thin lines indicate the magnetic flux lines. The higher the density of the magnetic flux lines, the higher the magnetic flux density. In addition, this relation is also pointed out by different colors. Magenta indicates a high magnetic flux density, cyan indicates a low magnetic flux density.

Furthermore, the tool can display the strength of the magnetic flux density along a user defined line. Therefore, a 30.0-mm-long line, parallel to the upper surface of the magnet, is drawn. The distance between the upper surface and the line is 11.4 mm. The resulting curve is shown in Figure 2. The DRV5053RA has a sensitivity of –40 mV/T. Therefore, to get the output signal of the DRV5053RA, the magnetic flux density must be multiplied by 40.

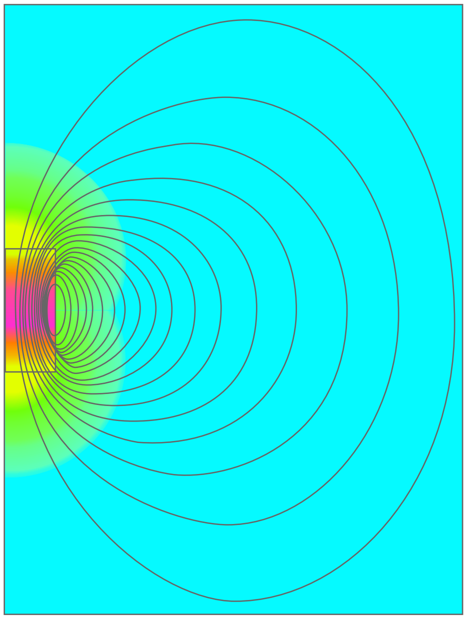

Figure 1. Simulated Magnetic Field of VACODYM® 863 AP

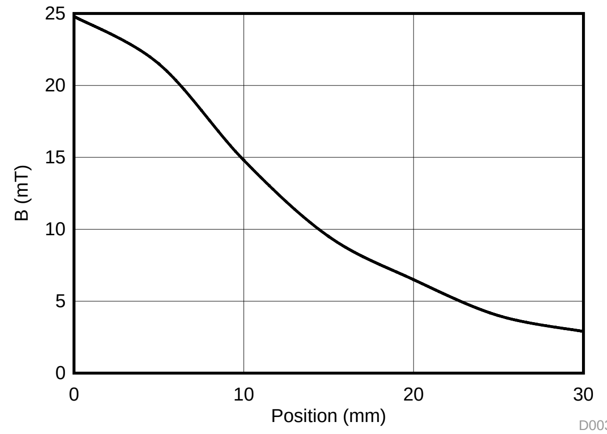

Figure 2. Simulated Magnetic Flux Density of VACODYM 863 AP

2.4 Going Further Simulating Magnetic Field for System Design Behind the Casing

The tool allowing to add materials with predefined characteristics, one can also use the tool to model the magnetic field behind stainless steal or plastics depending on the packaging constraints before starting the actual design.

3 System Description

The system is built with a Hall sensor whose output is linear in response to changing magnetic field (which needless to say given Section 2 is not linear with distance).

The output of the hall sensor is fed to the ADC of the MSP430, which samples this value and compares it to a pre-set value.

- If the ADC input is above the threshold, the switched output of the SN65HVD101 switches on.
- If the ADC input is below the threshold, the switched output of the SN65HVD101 switches off.
- If the ADC input is at the threshold (or within the hysteresis), the switched output of the SN65HVD101 does not switch.

The threshold is set by putting the system in the state where it should switch and press the push-button to "teach" the sensor the threshold.

3.1 Block Diagram

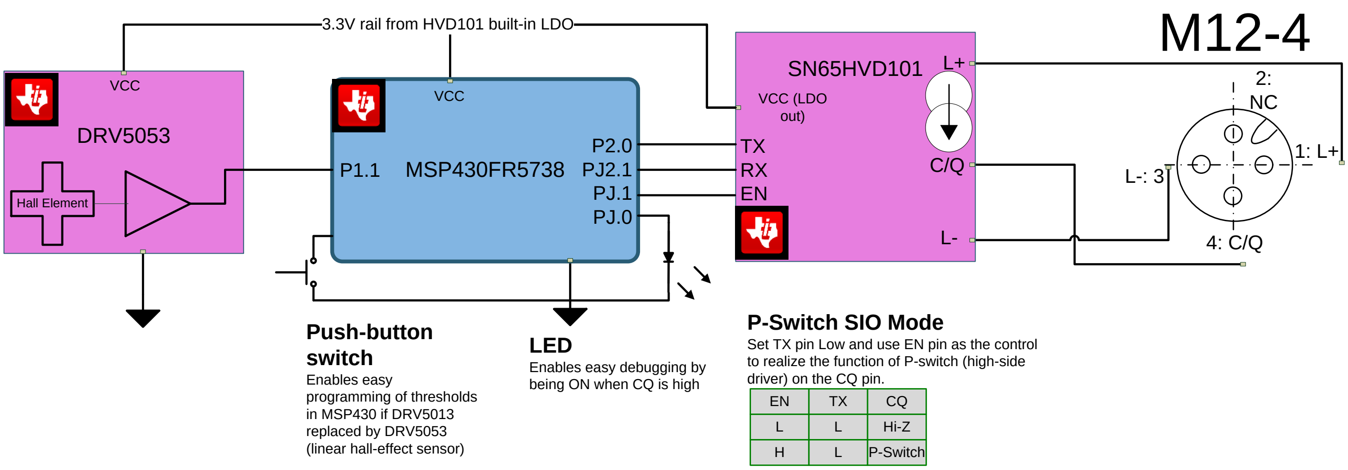

Figure 3. TIDA-00286 Block Diagram

3.2 DRV5053

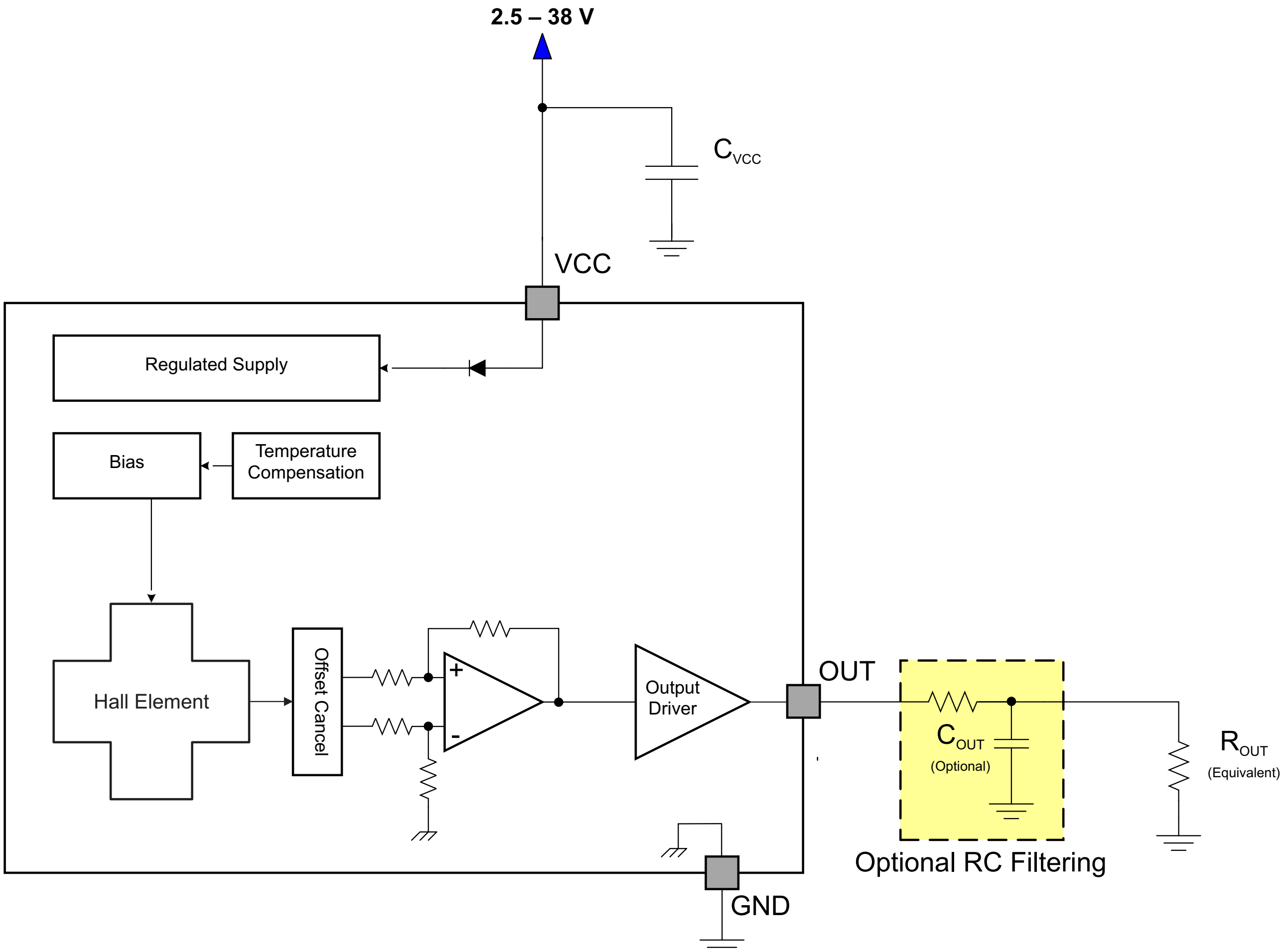

Figure 4. DRV5053 Block Diagram

Features:

- Linear output hall sensor
- Superior temperature stability
  - Sensitivity ±10% over temperature
- High sensitivity options:
  - –11 mV/mT (OA)
  - –23 mV/mT (PA)
  - –45 mV/mT (RA)
  - –90 mV/mT (VA)
  - 23 mV/mT (CA)
  - 45 mV/mT (EA)
- Supports a wide voltage range
  - 2.5 to 38 V
  - No external regulator required
- Wide operating temperature range
  - TA = –40°C to 125°C (Q)
- Amplified output stage
  - 2.3-mA sink, 300-μA source
- Output voltage: 0.2 to 1.8 V
  - B = 0 mT, OUT = 1 V
- Fast power-on: 35 μs
- Small package and footprint
  - Surface mount 3-pin SOT-23 (DBZ)
    - 2.92 × 2.37 mm
  - Through-hole 3-pin SIP (LPG)
    - 4.00 × 3.15 mm
- ƒBW bandwidth [1] 20 kHz

Protection features

- Reverse supply protection (up to –22 V)
- Supports up to 40-V load dump
- Output short circuit protection
- Output current limitation

(1) Bandwidth describes the fastest changing magnetic field that can be detected and translated to the output.

3.3 SN65HVD101

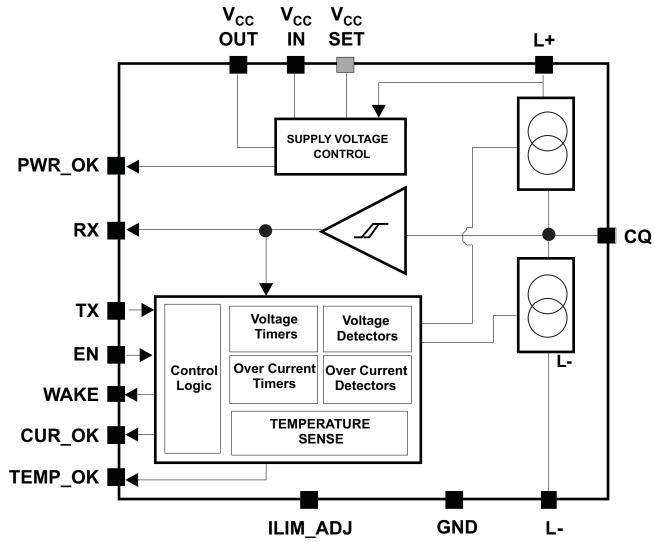

Figure 5. SN65HVD101 (IO-Link PHY for Device Nodes) Block Diagram

- Configurable CQ output: push-pull, high-side, or low-side for SIO mode
- Remote wake-up indicator
- Current limit indicator
- Power-good indicator
- Over temperature protection
- Reverse polarity protection
- Configurable current limits
- 9- to 36-V supply range
- Tolerant to 50-V peak line voltage
- 3.3-V and 5-V configurable integrated LDO
- 20-pin QFN package (4.0 × 3.5 mm)

3.4 MSP430FR5738

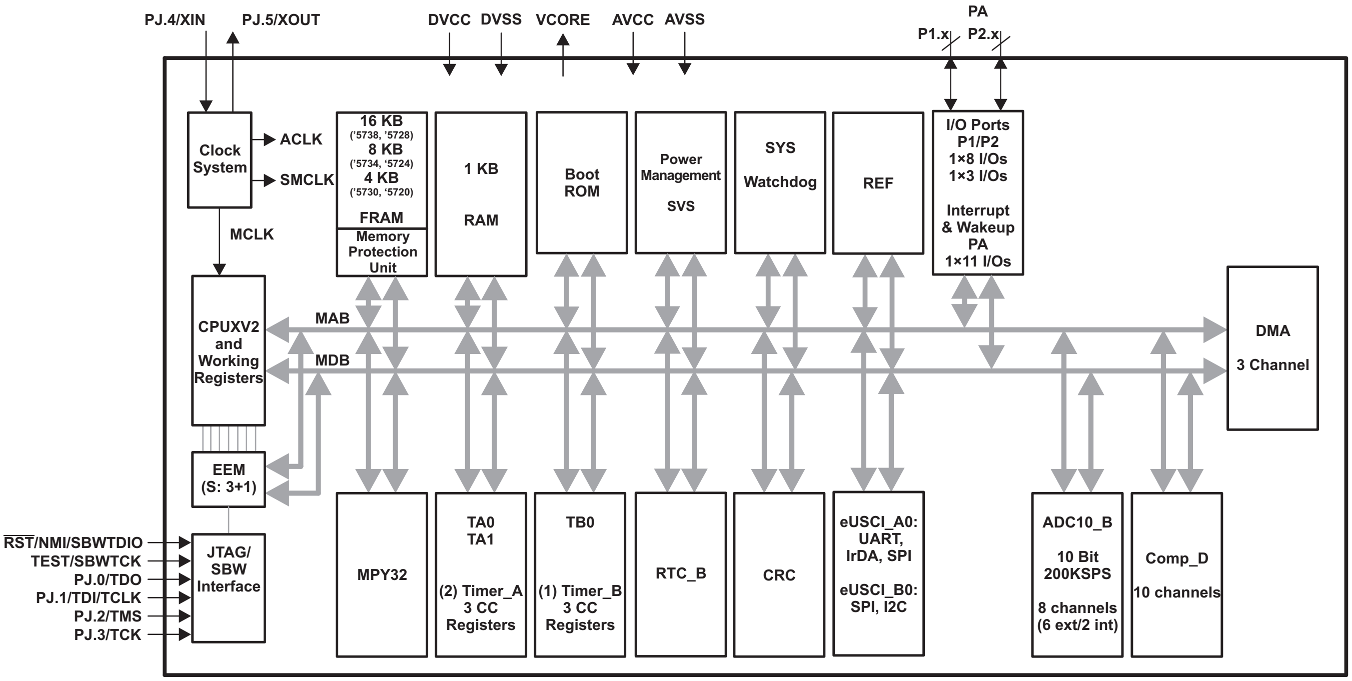

Figure 6. MSP430FR5738 Block Diagram

Embedded MCU 16-Bit RISC architecture up to 24-MHz clock:

- Wide supply voltage range (2 to 3.6 V)
- Optimized ultra low-power modes [81.4 µA/MHz in active and 320 nA in shutdown (LPM4.5)]
- Ultra low-power ferroelectric RAM
- 16-KB nonvolatile memory
- Ultra low-power writes
- Fast write at 125 ns per word (16KB in 1 ms)
- Built-in error coding and correction (ECC) and MPU
- Universal memory = program + data + storage
- 10^{15} write cycle endurance

Intelligent digital peripherals:

- 32-bit hardware multiplier (MPY)
- 3-channel internal DMA
- RTC with calendar and alarm functions
- 16-bit cyclic redundancy checker (CRC)
- High-performance analog
- Enhanced serial communication

4 Getting Started Hardware

4.1 Connecting Cable

Connect a standard M12 cable to connector J1 to provide power (over L+) and access the switch output (on C/Q).

4.2 JTAG Debugging and Firmware Upgrade

For MSP430 firmware updates, Code Composer Studio™ (CSS) is recommended. CCS is an integrated development environment (IDE) for Texas Instruments' (TI) embedded processor families. CCS comprises a suite of tools used to develop and debug embedded applications. CCS includes compilers for each of TI's device families, source code editor, project build environment, debugger, profiler, simulators, real-time operating system, and many other features. The intuitive IDE provides a single user interface taking the user through each step of the application development flow. For programming and debugging, the MSP430FR5738 implements an embedded emulation module (EEM). The EEM is accessed and controlled through either 4-wire JTAG mode or Spy-Bi-Wire mode. This reference design supports the Spy-Bi-Wire mode only. For more details on how the features of the EEM can be used together with CCS, see *Advanced Debugging Using the Enhanced Emulation Module,* (SLAA393).

The 2-wire interface is made up of the Spy-Bi-Wire test clock (SBWTCK) and Spy-Bi-Wire test data input/output (SBWTDIO) pins. The SBWTCK signal is the clock signal and a dedicated pin. In normal operation, this pin is internally pulled to ground. The SBWTDIO signal represents the data and is a bidirectional connection. To reduce the overhead of the 2-wire interface, the SBWTDIO line is shared with the RST/NMI pin of the device. For programming and debugging purposes, the SBWTCK, SBWTDIO, VCC, and GND from the debugger need to be connected on J1.

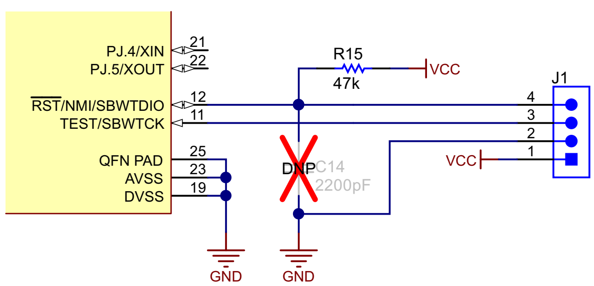

Figure 7. JTAG Connection (Pin 1 is Marked on PCB)

With the proper connections, an MSP430 Debugger Interface (such as the MSP-FET430UIF) can be used to program and debug code on the reference design.

CAUTION

Take special care during debugging to avoid damages due to different power domain in conflicts (IO-Link power and debugger tools power). Read this section carefully.

The SN65HVD101 integrates a linear voltage regulator, which supplies 3.3 V to the IO-Link demo board if a voltage in the range of 9 to 30 V is supplied to L+. Normally, the MSP430FR5738 is powered from this 3.3 V. If this local 3.3-V supply from the SN65HVD101 is used during debug, make sure the VCC_Target pin from the debugger interface is connected to VCC. If there is no local power and power from the debugger interface is used, make sure the VCC_Tool pin from the debugger interface is connected to VCC and disconnect the VCC_Target pin [see Figure 8 - Signal Connections for 2-Wire JTAG Communication (Spy-Bi-Wire)].

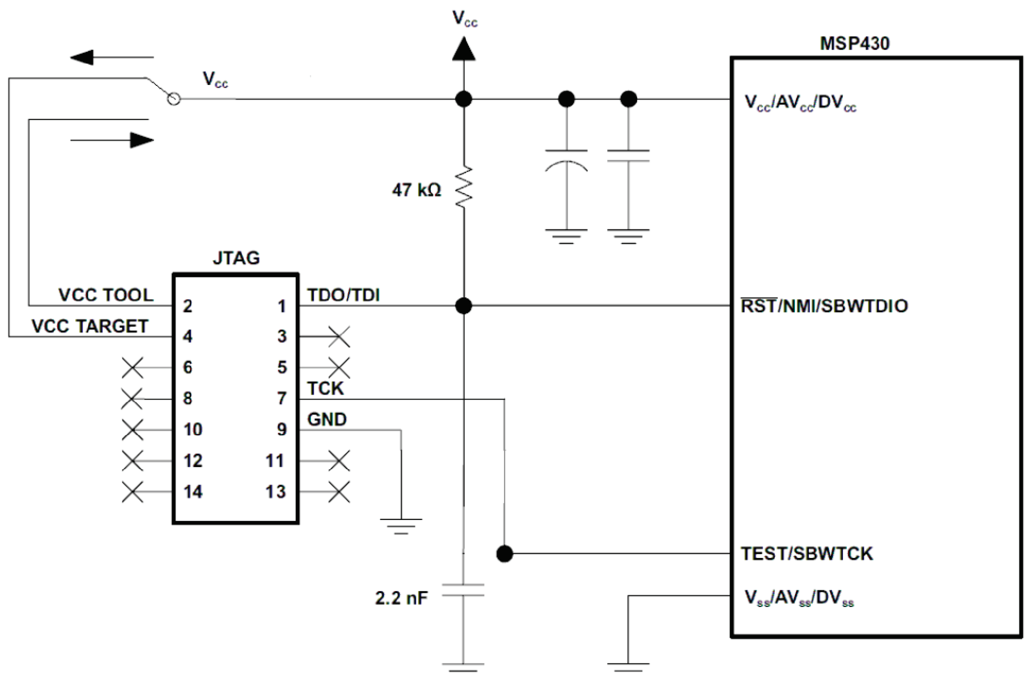

Figure 8. Signal Connections for 2-Wire JTAG Communication (Spy-Bi-Wire) View From Separate "Debugger Interface" Board

4.3 Programming the Proximity Threshold

The firmware comes by default with hysteresis and leverages the 10-bit ADC from the MSP430. With the 20 codes of hysteresis, the system is by default capable of resolving 50 different positions.

5 Getting Started Firmware

5.1 Overview

The firmware is providing a normally function (NO), which is when the magnetic field is below the programmed threshold the output will be open.

5.2 Programming the Threshold

To program the threshold, the magnetic field should be set to the desired strength either through Helmholtz coils or by having the target at the desired distance and the push-button on the PCB should be pressed.

5.3 Hysteresis

To avoid flickering when the magnetic field is close or at the target threshold, an hysterisis of 20 ADC codes has been programmed (as this corresponds to the system flickering from the characterization).

6 Test Setup

To provide a more complete characterization, a two-angle approach was selected. In the first approach, using Helmholtz coils, the current was set to increasing values in discrete steps, which allows a highly reproductible setup, and second approach with a more continuous measurement with a caliper to correlate the simulations results.

6.1 Earth Magnetic Field Considerations

The influence of the earth's magnetic field on the characterization of the TIDA-00286 is neglected. This can be done, because in Europe, the earth's magnetic field has a magnetic flux density of 48 µT, which is much lower than the magnetic flux density induced by the magnet or the coils.

6.2 Helmholtz Setup

For testing, the hardware was inserted in a Helmholtz coil (see Figure 9) whose key characteristics are:

- Homogeneity of the field within a 4×4×4-mm cube in the center on the coils is within 0.6%.
- The coil was characterized by the manufacturer over temp with their own magnetic sensor (air cooled) and shows change over temp <1% (due to mechanical dimension change of Helmholtz with a sensor)
- The coil key characteristic is 6 mT/A
- The lab power supply (Agilent U8031A with 30-V and 3-A capabilities and which was measured to have less than 1 mApp of ripple).

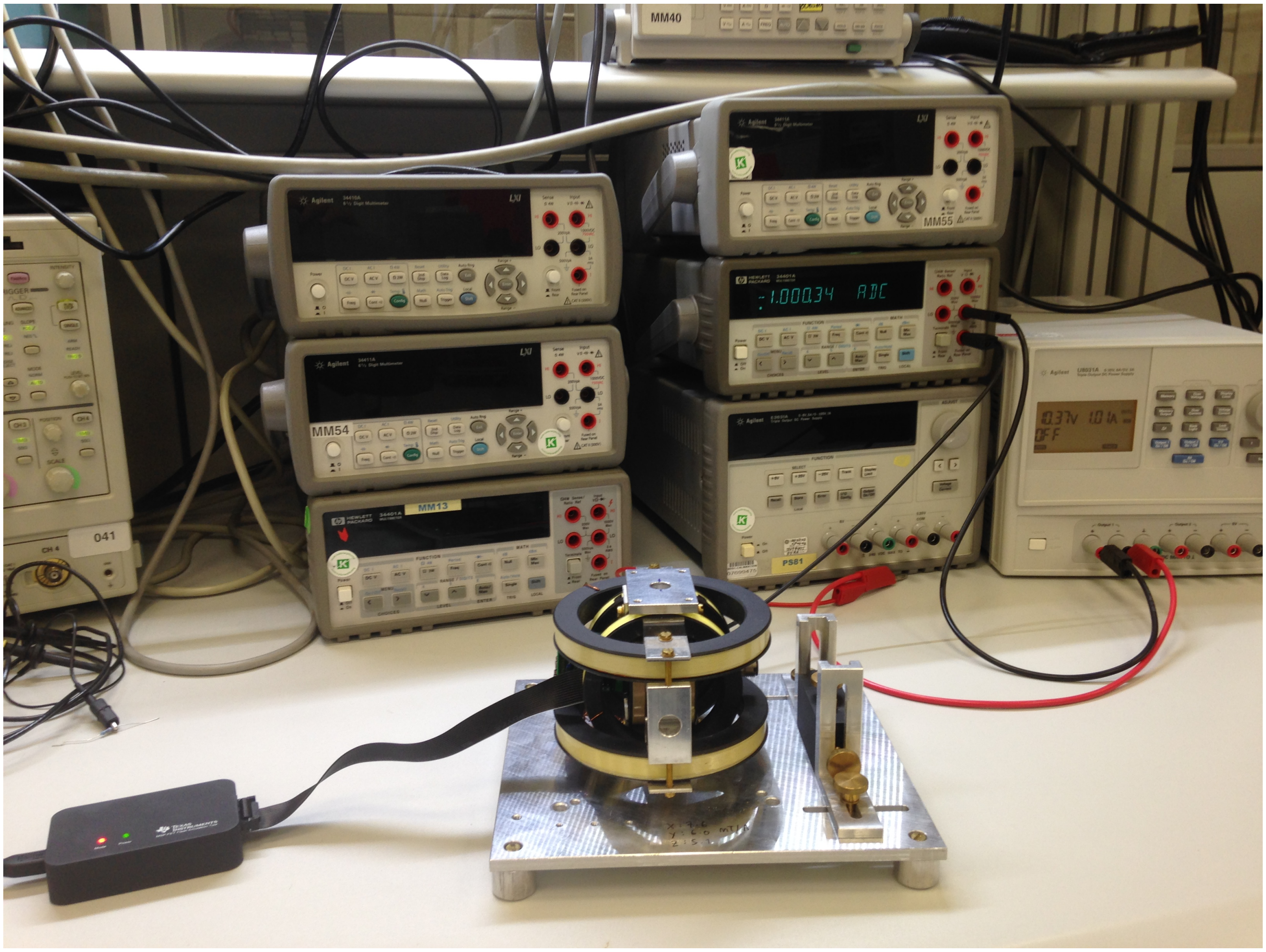

Figure 9. Helmholtz Lab Setup

The current in the coil was changed and readings of the ADC inputs value at different magnetic fields are reported in Section 7.

6.3 Caliper Setup

To characterize the DRV5053RA the following test setup is built up. The DRV5053RA is placed on a PCB that is fixed onto the lower bar of a caliper. Then, a disc magnet is positioned underneath the moving range of the caliper. The disc magnet is from Vacuumschmelze GmbH & Co. KG. The series number is VACODYM 863 AP. The magnetic remanence of the used magnet is 1.21 T, 6-mm high, and has a radius of 5 mm. The distance between the magnet surface and the sensor amounts about 11.4 mm.

7 Test Data

7.1 Helmholtz Setup

Figure 10 shows

- “Hall output reading by MSP430 ADC”
- “Error peak-peak in Tesla”

The first curve is the average over 5000 ADC readings of the codes the ADC renders (10-bit ADC) and the code then is translated back in equivalent voltage. Specifically, a full-scale ADC reading is 2^{10} and is equivalent to 2 V. Those 5000 ADC readings were generated at different currents flowing through the coils, which generated the magnetic field in the x-axis.

The second curve, “error peak-peak in Tesla”, is the difference between the two most extreme codes within the 5000 ADC readings and translated back into equivalent magnetic field to show that the error takes into account the entire signal chain from the Hall sensor, the Hall sensor on-chip signal conditioning, the PCB filtering, and the ADC noise contributions.

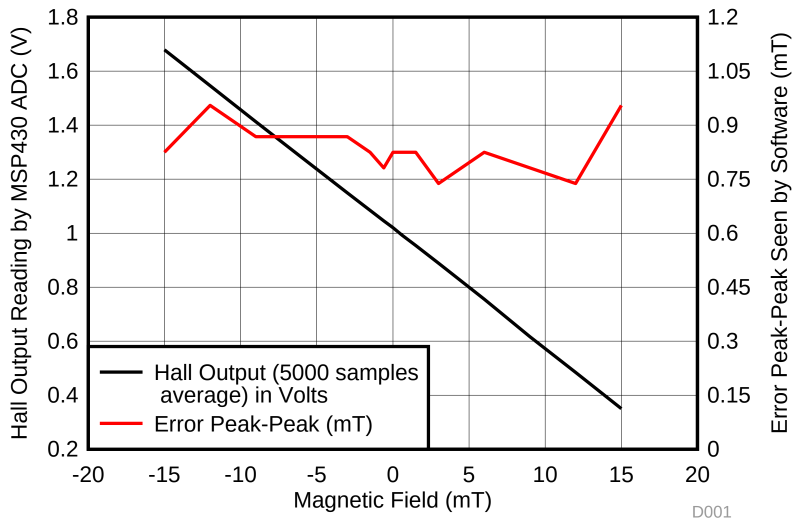

Figure 10. System Characterization

7.2 Caliper Setup

The testing protocol followed is as follows:

1. Position the sensor over the middle of the magnet.
2. Set the scale of the caliper to 0.00 mm.
3. Move the sensor board from 0.00 to –25.00 mm
4. Then move in the same steps from 0 to 25 mm
5. Record the output value of the Hall sensor for every position.
6. The resulting characteristic of the sensor are shown in Figure 11.

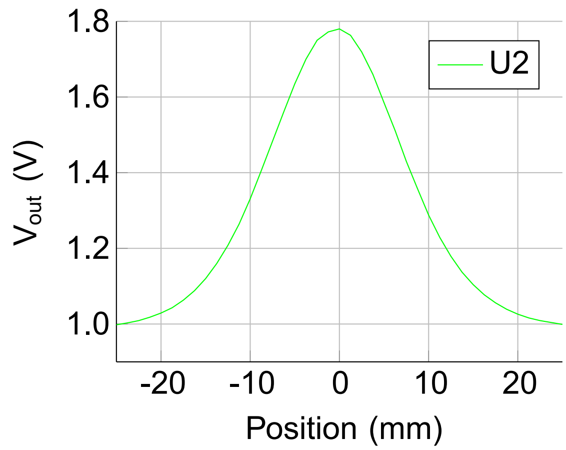

Figure 11. Caliper Characterization Results

7.3 Power Consumption

The power consumption of the system is plotted below, where the L+ voltage was varied between 18 and 33 V. Two curves are visible, one when the LED was *OFF* (equivalent to the field has been below B_{OP} of DRV5053) and LED *ON* (when the field has been above B_{RP}).

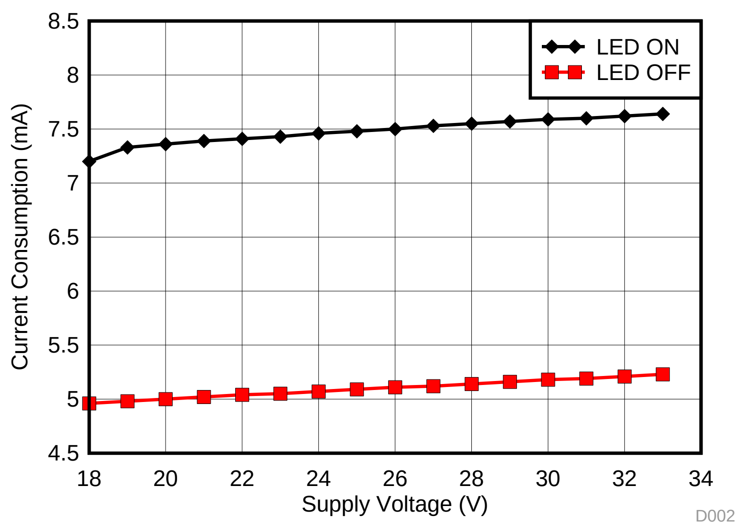

Figure 12. Power Consumption Graphs

7.4 Finite Element Configuration File

The below listing should be copied into a file called *FEMM single magnet.FEM* and loaded in the tool to reproduce the details of what is exposed in Section 2.3.

```
[Format] = 4.0
[Frequency] = 0
[Precision] = 1e-008
[MinAngle] = 30
[Depth] = 1
[LengthUnits] = millimeters
[ProblemType] = axisymmetric
[Coordinates] = cartesian
[ACSolver] = 0
[Comment] = "Add comments here."
[PointProps] = 0
[BdryProps] = 1
  <BeginBdry>
    <BdryName> = "New Boundary"
    <BdryType> = 0
    <A_0> = 0
    <A_1> = 0
    <A_2> = 0
    <Phi> = 0
    <c0> = 0
    <c0i> = 0
    <c1> = 0
    <c1i> = 0
    <Mu_ssd> = 0
    <Sigma_ssd> = 0
  <EndBdry>
[BlockProps] = 5
  <BeginBlock>
    <BlockName> = "Air"
    <Mu_x> = 1
    <Mu_y> = 1
    <H_c> = 0
    <H_cAngle> = 0
    <J_re> = 0
    <J_im> = 0
    <Sigma> = 0
    <d_lam> = 0
    <Phi_h> = 0
    <Phi_hx> = 0
    <Phi_hy> = 0
    <LamType> = 0
    <LamFill> = 1
    <NStrands> = 0
    <WireD> = 0
    <BHPoints> = 0
  <EndBlock>
```

```
<BeginBlock>
    <BlockName> = "VD 863 AP"
    <Mu_x> = 1
    <Mu_y> = 1
    <H_c> = 925000
    <H_cAngle> = 0
    <J_re> = 0
    <J_im> = 0
    <Sigma> = 0
    <d_lam> = 0
    <Phi_h> = 0
    <Phi_hx> = 0
    <Phi_hy> = 0
    <LamType> = 0
    <LamFill> = 1
    <NStrands> = 0
    <WireD> = 0
    <BHPoints> = 0
<EndBlock>
<BeginBlock>
    <BlockName> = "VD 863 AP 2"
    <Mu_x> = 1
    <Mu_y> = 1
    <H_c> = 1110000
    <H_cAngle> = 0
    <J_re> = 0
    <J_im> = 0
    <Sigma> = 0
    <d_lam> = 0
    <Phi_h> = 0
    <Phi_hx> = 0
    <Phi_hy> = 0
    <LamType> = 0
    <LamFill> = 1
    <NStrands> = 0
    <WireD> = 0
    <BHPoints> = 0
<EndBlock>
<BeginBlock>
    <BlockName> = "416 stainless steel, annealed"
    <Mu_x> = 1
    <Mu_y> = 1
    <H_c> = 0
    <H_cAngle> = 0
    <J_re> = 0
    <J_im> = 0
    <Sigma> = 1.74
    <d_lam> = 0
    <Phi_h> = 0
    <Phi_hx> = 0
    <Phi_hy> = 0
    <LamType> = 0
    <LamFill> = 1
    <NStrands> = 0
    <WireD> = 0
    <BHPoints> = 33
```

0.0.	
0.20778995919879328	320.92999999999995
0.22364931371099023	331.02666666666664
0.25084135512504779	348.56666666666666
0.26171716173194137	355.83999999999997
0.28346935718756683	370.84999999999997
0.2889075243847965	374.6966666666666
0.41218760024480688	470.25
0.62566054494422463	660.92666666666662
0.68005862210630241	717.75333333333322
0.78252281053007089	837.79999999999984
0.80020925624997319	864.15000000000009
0.95816502937412396	1165.8333333333333
1.0767969774200417	1509.5666666666666
1.1100488305016618	1656.9333333333329
1.2055703265999278	2284.1333333333332
1.2385842209600626	2613.5
1.3726454443074343	4969.9666666666662
1.4275581497186043	6783.833333333333
1.5422692199452028	12124.333333333332
1.5580865944646081	13172.666666666666
1.5620671785059184	13449
1.6334236260295694	21451.666666666664
1.6754034599026606	30215.666666666664
1.6932013471857443	36049.666666666664
1.7139092459532073	44836
1.7383144421097252	58739.666666666664
1.76404286494438 76959	
1.8507986277495354	143556.66666666666
1.8769989795155597	164326.66666666666
2.0216195572312698	279173.33333333331
2.0403266942858456	294060
2.0765429743964292	322880

<EndBlock>
<BeginBlock>
<BlockName> = "2.5mm"
<Mu_x> = 1
<Mu_y> = 1
<H_c> = 0
<H_cAngle> = 0
<J_re> = 0
<J_im> = 0
<Sigma> = 58
<d_lam> = 0
<Phi_h> = 0
<Phi_hx> = 0
<Phi_hy> = 0
<LamType> = 3
<LamFill> = 1
<NStrands> = 1
<WireD> = 2.5
<BHPoints> = 0
<EndBlock>

[CircuitProps] = 0
[NumPoints] = 10

0	–6	0	0		
0	6	0	0		
5	–6	0	0		
5	6	0	0		
0	50	0	0		
0	–50	0	0		
0	26	0	0		
0	43.5	0	0		
0.20000000000000001		20.100000000000001		0	0
15.199999999999999		19.899999999999999		0	0

[NumSegments] = 9

0	1	–1	0	0	0
3	1	–1	0	0	0
3	2	–1	0	0	0
2	0	–1	0	0	0
5	0	–1	0	0	0
1	6	–1	0	0	0
7	4	–1	0	0	0
7	6	–1	0	0	0
8	9	–1	0	0	0

[NumArcSegments] = 1

5	4	180	1	1	0	0

[NumHoles] = 0
[NumBlockLabels] = 2

23	19.100000000000001	1	–1	0	0	0	1	0		
1.6000000000000001	–0.80000000000000004			3	–1	0	90	0	1	0

8 Design Files

8.1 Schematics

To download the schematics, see the design files at TIDA-00286.

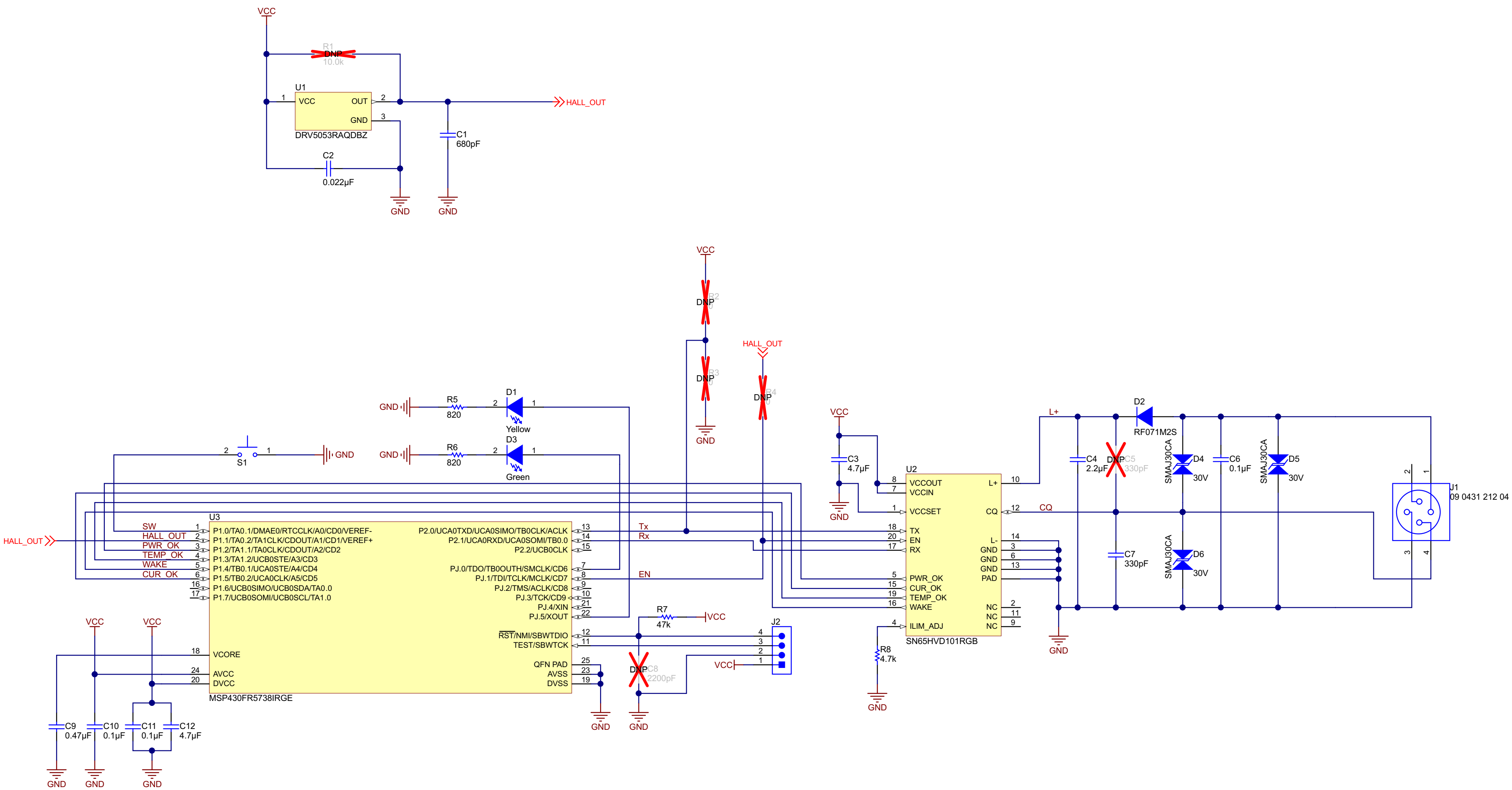

Figure 13. TIDA-00286 Schematic

8.2 Bill of Materials

To download the bill of materials (BOM), see the design files at TIDA-00286.

Table 2. BOM

ITEM	DESIGNATOR	QTY	VALUE	PARTNUMBER	MANUFACTURER	DESCRIPTION	PACKAGE REFERENCE
1	C1	1	680 pF	GRM155R71H681KA01D	MuRata	CAP, CERM, 680 pF, 50 V, ±10%, X7R, 0402	0402
2	C2	1	0.022 µF	GRM155R71C223KA01D	MuRata	CAP, CERM, 0.022 µF, 16 V, ±10%, X7R, 0402	0402
3	C3, C12	2	4.7 µF	C1005X5R0J475M050BC	TDK	CAP, CERM, 4.7 µF, 6.3 V, ±20%, X5R, 0402	0402
4	C4	1	2.2 µF	GRM32ER72A225KA35L	MuRata	CAP, CERM, 2.2 µF, 100 V, ±10%, X7R, 1210	1210
5	C6	1	0.1 µF	12061C104JAT2A	AVX	CAP, CERM, 0.1 µF, 100 V, ±5%, X7R, 1206	1206
6	C7	1	330 pF	GRM155R72A331KA01D	MuRata	CAP, CERM, 330 pF, 100 V, ±10%, X7R, 0402	0402
7	C9	1	0.47 µF	GRM155R60J474KE19D	MuRata	CAP, CERM, 0.47 µF, 6.3 V, ±10%, X5R, 0402	0402
8	C10, C11	2	0.1 µF	C1005X5R0J104K	TDK	CAP, CERM, 0.1 µF, 6.3 V, ±10%, X5R, 0402	0402
9	D1	1	Yellow	LY L29K-J1K2-26-Z	OSRAM	LED, Yellow, SMD	LED, 1.3 × 0.65 × 0.8 mm
10	D2	1	200 V	RF071M2S	Rohm	Diode, Ultrafast, 200 V, 1 A, SOD-123	SOD-123
11	D3	1	Green	LG L29K-G2J1-24-Z	OSRAM	LED, Green, SMD	1.7 × 0.65 × 0.8 mm
12	D4, D5, D6	3	30 V	SMAJ30CA	Bourns	Diode, TVS, Bi, 30 V, 400 W, SMA	SMA
13	J1	1		09 0431 212 04	Binder-Connector	M12 Socket, 4Pos, TH	M12 Conn D12x14.3
14	J2	1		850-10-004-40-001000	Mill-Max	Header, 4×1, 50 mil, R/A, SMT	Header, 50 mil, R/A,SMT
15	R5, R6	2	820 Ω	CRCW0402820RJNED	Vishay-Dale	RES, 820 Ω, 5%, 0.063 W, 0402	0402
16	R7	1	47 kΩ	CRCW040247K0JNED	Vishay-Dale	RES, 47 kΩ, 5%, 0.063 W, 0402	0402
17	R8	1	4.7 kΩ	CRCW04024K70JNED	Vishay-Dale	RES, 4.7 kΩ, 5%, 0.063 W, 0402	0402
18	S1	1		SKRKAEE010	Alps	Switch, Push Button, SMD	2.9 × 2 × 3.9 mm SMD
19	U1	1		DRV5053RAQDBZ	Texas Instruments	Analog-Bipolar Hall Effect Sensor, –40 mV/mt, –40°C to 125°C, DBZ0003A	DBZ0003A
20	U2	1		SN65HVD101RGB	Texas Instruments	IO-LINK PHY for Device Nodes, RGB0020A	RGB0020A
21	U3	1		MSP430FR5738IRGE	Texas Instruments	24-MHz Mixed Signal Microcontroller, 1024 B SRAM and 17 GPIOs, –40°C to 85°C, RGE0024G	RGE0024G

Table 2. BOM (continued)

ITEM	DESIGNATOR	QTY	VALUE	PARTNUMBER	MANUFACTURER	DESCRIPTION	PACKAGE REFERENCE
22	C5	0	330 pF	GRM155R72A331KA01D	MuRata	CAP, CERM, 330 pF, 100 V, ±10%, X7R, 0402	0402
23	C8	0	2200 pF	GRM155R70J222KA01D	MuRata	CAP, CERM, 2200 pF, 6.3 V, ±10%, X7R, 0402	0402
24	R1	0	10.0 kΩ	CRCW040210K0FKED	Vishay-Dale	RES, 10.0 kΩ, 1%, 0.063 W, 0402	0402
25	R2, R3, R4	0	0	CRCW04020000Z0ED	Vishay-Dale	RES, 0 Ω, 5%, 0.063W, 0402	0402

8.3 Layer Plots

To download the layer plots, see the design files at TIDA-00286.

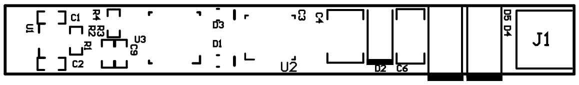

Figure 14. Top Overlay

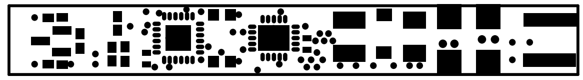

Figure 15. Top Solder Mask

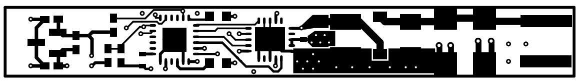

Figure 16. Top Layer

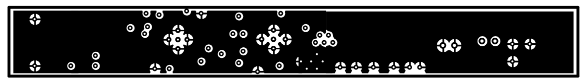

Figure 17. Mid Layer 1

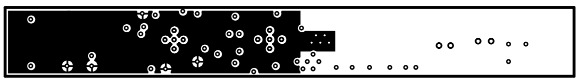

Figure 18. Mid Layer 2

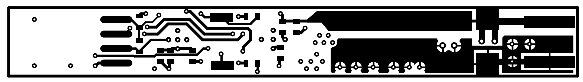

Figure 19. Bottom Layer

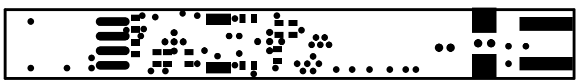

Figure 20. Bottom Solder Mask

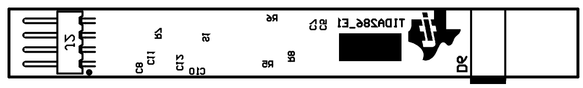

Figure 21. Bottom Overlay

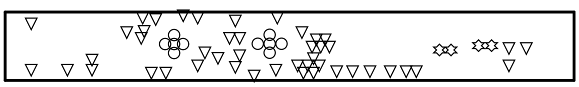

Figure 22. Drill Drawing

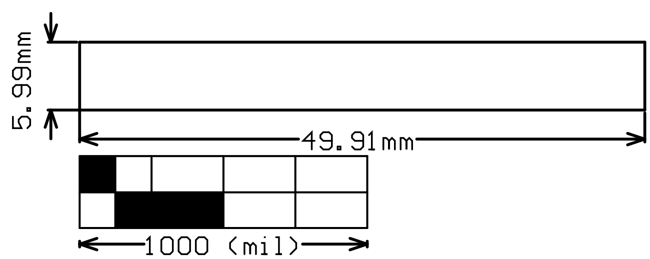

Figure 23. Board Dimensions

8.4 Altium Project

To download the Altium project files, see the design files at TIDA-00286.

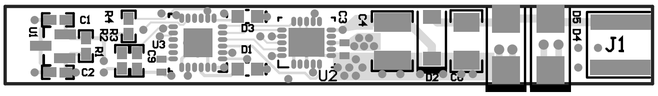

Figure 24. Altium Project Top

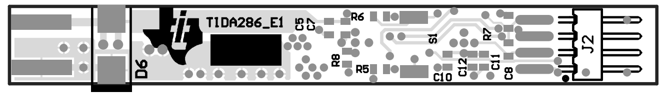

Figure 25. Altium Project Bottom

8.5 Assembly Drawings

To download the assembly drawings, see the design files at TIDA-00286.

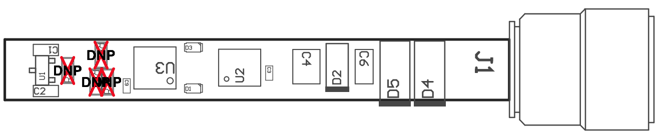

Figure 26. Top Assembly Drawing

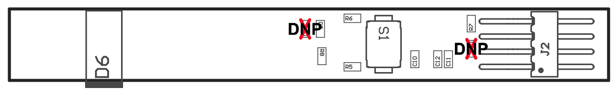

Figure 27. Bottom Assembly Drawing

8.6 Software Files

To download the software files, see the design files at TIDA-00286.

9 References

1. IEC, IEC 61131-2 Programmable controllers — Part 2: Equipment requirements and tests, 2007.
2. Community, IO-LINK, "IO-Link Interface and System Specification v1.1.2," *IO-LINK Community*, 2013, pp. 51–52.
3. Texas Instruments, SN65HVS882 Datasheet. "Industrial 8-Digital-Input Serializer" Jan 2009. (SLAS601) [Accessed 05/06/2014].
4. E. Ramsden, Hall-Effect Sensors: Theory and Application, Second Edition, Newnes, 2006.
5. Texas Instruments, TIDA-00188 Design Guide. "Turnkey IO-Link Sensor Transmitter" (TIDU259A).
6. K. Iniewski. "Optical, Acoustic, Magnetic, and Mechanical Sensor Technologies. Devices, Circuits, and Systems." *Taylor & Francis*, 2012. ISBN: 9781439869758.
7. D.C. Meeker. femm 4.2, Finite Element Method Magnetics. http://www.femm.info [Accessed on 09/08/2014].
8. Slawomir Tumanski. Handbook of magnetic measurements. 2011. ISBN: 978-1-283- 25744-2.
9. Mats G. Larson. "The Finite Element Method: Theory, Implementation, and Applications. Ed. by Fredrik Bengzon." *Texts in Computational Science and Engineering*. Berlin, Heidelberg: Springer, 2013. ISBN: 978-3-642-33287-6.

10 Terminology

SIO— Standard input output (digital switching mode) [IEC 61131-2]; also referred to as switch output (NPN or PNP)

SDCI— Single-drop digital communication interface

Hall effect— A Hall-effect sensor is a transducer leveraging certain material whose property is to generate a voltage proportional to the magnetic field they are exposed to

Sensitive axis— An axis going through and orthogonal to the plane where the Hall-effect sensing element has been placed

11 About the Author

MATTHIEU CHEVRIER is a systems architect at Texas Instruments where he is responsible for defining and developing solutions for the industrial segment. Matthieu brings to this role his extensive experience in embedded system designs in both hardware (such as power management and mixed signal) and software (such as low level drivers, RTOS, and compilers). Matthieu earned his master of science in electrical engineering (MSEE) from Supélec, an Ivy League university in France. Matthieu holds patents from IPO, EPO, and USPTO.

ALEXANDRE WEILER is a systems architect at Texas Instruments where he is responsible for developing reference design solutions for the industrial segment. Alexandre brings to this role his extensive experience in high-speed digital, low-noise analog, and RF system-level design expertise. Alexandre earned his diploma in electrical engineering [Dipl.-Ing. (FH)] from University of Applied Science in Karlsruhe, Germany.

Mailing Address: Texas Instruments, Post Office Box 655303, Dallas, Texas 75265